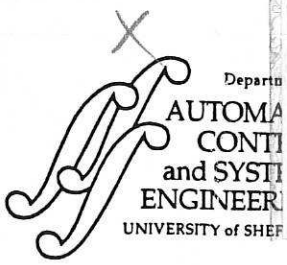

DESIGN AND DEVELOPMENT OF A LABORATORY-SCALE SINGLE-LINK FLEXIBLE MANIPULATOR SYSTEM

M O Tokhi and A K M Azad

Department of Automatic Control and Systems Engineering,
The University of Sheffield, Mappin Street, Sheffield, S1 3JD, UK.

Tel: + 44 (0)114 2825136.
Fax: + 44 (0)114 2731 729.
E-mail: O.Tokhi@sheffield.ac.uk.

Research Report No. 594

August 1995

Abstract

This paper presents the design and development of a laboratory facility constituting a constrained planar flexible manipulator system. The system is designed for experimental investigations within research programmes involving flexible manipulator systems. An outline of a generic design procedure for flexible manipulator systems is given. The design criteria developed through this procedure account for the strength and stiffness of the manipulator and the required transducers and instrumentation. These are considered in detail and the system designed accordingly. Finally, practical problems encountered are highlighted and methods of dealing with such problems are presented and discussed.

CONTENTS

LIST OF FIGURES

1 Introduction

The increasing demand for system automation has recently necessitated the employment of robots in various applications. The major factor which contributes largely to performance limitations of the robot is the limited capability of its control system especially in applications requiring high speed and/or large payloads. Recently, the demand for light weight elastic manipulators has increased as they improve the speed of operation and handle larger payloads in comparison to rigid manipulators with the same actuator capabilities. However, their structural flexibility results in oscillatory behaviour in the system. Various types of flexible manipulator are used in experimental and prototype applications. To design a flexible manipulator efficiently, whether intended for a specific application or for a range of applications, several factors need to be considered. These include the strength and flexibility of the manipulator, maximum speed and acceleration capability, payload requirement, choice of suitable actuator and sensing equipment for the control mechanisms intended to be employed. The problem of oscillatory behaviour due to manipulator flexibility has traditionally been solved by mechanically stiffening the manipulator. However, this leads to an increase in the weight of the manipulator. Thus, a conventional industrial robot does not achieve the objective of the lighter weight requirement of the flexible manipulator. The issue of flexible manipulator design and control thus primarily caters for the design of controllers to either compensate for the structural flexibility or to be robust in the presence of structural flexibility.

It has been shown that using joint position and velocity sensors in a feedback control scheme for a rigid robot is adequate to ensure satisfactory performance (Khosla and Kanade, 1988). However, these sensors may not be sufficient to provide the necessary information for the control of elastic behaviour in a robot. In addition to measuring joint position and velocity, it is desirable to obtain the state of the end-point. Although the deflection information of the manipulator can be theoretically determined if the dynamic model of the system is available, this will require high computing power and speed for on-line computation in addition to the uncertainties usually associated with formulating the dynamic model of the flexible manipulator. This argument for control purposes leads to the

requirement of a suitable measuring system at the free-end (end-point) of the flexible manipulator.

This paper presents the design of a laboratory facility for experimental study of a constrained planar single-link flexible manipulator and verification of controller designs. Similar experimental manipulators have been constructed in the past (Hastings and Ravishankar, 1988). The principal originality of the design presented here is that the deflection of the flexible manipulator is measured and controlled using an accelerometer at the end-point.

2 Design procedure

A preliminary design procedure for a flexible manipulator system is presented in this section. A single-link flexible manipulator incorporating a payload mass at the end-point and a lumped inertia at the hub end is considered. The design procedure presented can also be applied to a manipulator having more than one joint.

The main purpose here is to relate a set of criteria which are useful in the design procedure. These include postitional accuracy of end-point, allowable payload mass, maximum joint (hub) velocity, maximum hub acceleration and operating bandwidth of the manipulator. This will lead to the preliminary results of the manipulator parameters. The actuating system is also studied and incorporated into the design procedure. Moreover, the significance of flexibility for the range of specifications will also be indicated.

Figure 1 shows a flow chart of the design procedure. The initial values or given parameters are length of the manipulator, payload mass at the end-point, lumped inertia at the hub, angle of movement and travel time (or velocity and acceleration). The results of the procedure will be criteria concerning the required DC motor (torque capacity, armature inertia, speed/torque characteristics, power dissipation etc.), gear ratio and size of the flexible manipulator.

3 Strength and stiffness

Manipulator strength and stiffness are qualitatively affected by a number of parameters including payload mass, material density, length and cross section of the manipulator. Varying one of these parameters so as to make the manipulator stronger results in a stiffer manipulator. Other parameters directly affecting only strength include the maximum allowable stress for the manipulator material, inertial loading from accelerating the manipulator and its payload, and the gravity or other constant body forces present in the environment. Stiffness is characterised by the natural frequencies, and its magnitude is additionally affected by the value of the Young modulus for the material used.

For the single-link manipulator proposed here, there are only two parameters, namely, thickness and width, that can be altered to increase its strength. The minimum thickness, as discussed later, will limit the stability of the manipulator.

A schematic representation of the proposed constrained planar single-link flexible manipulator system is shown in Figure 2, where E, I, l, ρ, M_p and I_h are the Young modulus, area moment of inertia, length, mass density per unit length, payload mass and hub inertia of the manipulator respectively. The manipulator can, thus, be considered as a pinned-free flexible beam with a lumped inertia at the hub, which can bend freely in the horizontal plane but is stiff in vertical bending and torsion. Shear deformation, rotary inertia and effect of axial force are assumed to be negligible. For a given value of payload mass at the end-point and a desired linear acceleration at the centre of gravity of the payload mass, the desired moment at the hub can be calculated using (Book, 1974)

$$\sigma = \alpha M_p w + \alpha M_p l + \frac{\rho}{2}\left[\frac{\alpha - g}{l + w} + g\right] l^2 - \frac{\rho(\alpha - g)}{6(l + w)} l^3 + \frac{I_h \alpha}{l + w}$$

where,

σ = required moment at the hub.

α = linear acceleration at the centre of gravity of the payload mass.

w = offset between the centre of gravity of the payload mass and the end-point of the manipulator.

g = acceleration due to gravity.

For a given flexible manipulator, the maximum torque which can be applied to the hub is given by

$$\tau_{max} = \frac{\sigma_{max} I}{C}$$

where,

τ_{max} = maximum applied torque.

σ_{max} = maximum tensile stress (without changing the shape). This depends upon the material used in constructing the flexible manipulator.

C = half the thickness of the manipulator.

For the manipulator to be strong enough to handle the desired torque, the relation

$$\sigma_{max} \geq \sigma \qquad (1)$$

must be satisfied. Note in equation (1) that equality applies to the optimum structure of the manipulator. It follows from equation (1) that the minimum thickness of the flexible manipulator depends upon the amount of torque required to be applied at the hub, i.e. upon the linear acceleration at the centre of gravity of the payload mass. The safety factor for the manipulator design can, thus, be defined as

$$SF = \frac{\sigma_{max}}{\sigma}$$

For optimum design, the safety factor is unity. It follows from the above that the thickness and type of material allow varying the strength of a flexible manipulator. These two parameters are combined with load specifications (length of the manipulator and payload) to set two design parameters, namely, σ and τ_{max}.

4 Transducers and instrumentation

It was decided at the design stage to provide the manipulator with a range of sensors comparable to those which might be used with a flexible manipulator in an industrial

environment. A realistic set of measurements were considered to be the position and velocity at the hub, acceleration at the end-point and strain along the length of the manipulator. The required transducers and instrumentation can be grouped as (i) drive actuator, (ii) drive amplifier, (iii) hub angle sensor and processing circuit, (iv) hub velocity sensor and amplifier, (v) strain gauge and amplifier and (vi) accelerometer and amplifier. These are presented below.

4.1 Drive actuator

One of the important factors in the design is the selection of a suitable actuator to drive the manipulator. Three types of drive actuators are commonly used: shape memory actuator (SMA), fluid power driver and electric motor. The SMA represents a new class of actuators made of a nickel titanium alloy called Nitinol, which is capable of transforming thermal energy into mechanical work by using pulsed DC current (Hirose, et.al, 1986; Yeager, 1984). These type of actuators have several advantages, such as simplicity of mechanisms, cleanliness, silent actuation, distributed actuation capability, sensing ability and low driving voltage. At present there are three major difficulties associated with the SMA which prevent its widespread use (Furuya and Shimada, 1991). Firstly it has low efficiency in transforming electrical power into motion. In general, the efficiency of a conventional robot system is about 40 to 50%, while that of the SMA robot is only 5 to 6%. Secondly, the fatigue and shape memory degradation following the continued use of an SMA. Thirdly, its response speed is determined by the heating and cooling effects. Despite all its disadvantages, the SMA has successfully been used in some applications, particularly in harsh environments, such as ocean water, nuclear and medical applications (Furuya, et. al, 1987; Hirose, et. al, 1984).

Fluid power drivers for robots are mainly used in the form of full servo controlled hydraulic systems for heavy duty operations (for more than 5 hp actuators) and non-servo controlled pneumatic systems for high speed and light duty operations (Klafter, et. al, 1989). Hydraulic type actuators are known to be in use for flexible manipulator

applications (Chang and Cannon, 1990). The inherent disadvantages of hydraulic systems include fluid leakage and bulky support equipment, noisy operation, temperature effect on the fluid used and a complex servo controlled system. These systems are highly nonlinear within the operating range of flexible manipulators and thus need to be considered during the controller design. Despite all these disadvantages, hydraulic actuators are used in explosive atmospheres such as in paint spray booths.

Pneumatic drivers are the simplest of all. However, with these drives, due to the compressibility of the air, it is difficult to control fine motion and specially vibration in the case of a flexible manipulator system (Klafter, et. al, 1989).

Among electric motors a printed circuit armature type permanent magnet DC motor is favoured to drive the flexible manipulator. The difference in construction enables printed circuit motor to deliver a level of performance, in both incremental motion and continuous speed applications, which is not attainable with conventional iron-core and moving coil motor designs (Critchlow, 1985; PMI Motion Technologies, 1988). The printed armature gives a smooth torque output even at low speeds and the absence of magnetic material in the armature gives a linear torque/current relationship. The armature has a low inertia. Together with the low inertia of the flexible manipulator, this means that most of the motor energy is being used to perform useful work. This is a desirable feature for a flexible manipulator.

In addition to performance advantages, printed circuit motors have a unique compact shape that can be an attractive alternative when solving tight packing problems. From a performance viewpoint, this shape provides closer physical coupling and better torsional stiffness. These key factors can optimise the mechanical design of a flexible manipulator system.

There are two other types of motors, namely, stepper motor and brushless DC motor, which could also be used in flexible manipulators (Electrocraft Corporation, 1985). Stepper motors are very useful and economical, due to their inherent control of position. However, problems associated with the currently available stepper motors include lack of availability of variety of step angles, fixed step angles, slew speed problems, jerky speed

and inability to handle large inertial loads. Due to electronic commutation, brushless motors do not suffer from mechanical wear except in the motor bearings (Inland Motors, 1985). However, they are expensive and their life expectancy is limited by the reliability of the electronic commutation (Electrocraft Corporation, 1985). Moreover, these require a controller with a more complex configuration than that for a brush-type motor. In the proposed flexible manipulator system, the power requirements for the drive motor are not too high and with the printed circuit armature the amount of self induced emf is much lower than the iron core one. Thus, the commutation arcing interference can be eliminated by using suitable bypass capacitors and properly isolating the electronic circuits dealing with sensitive feedback signals.

The objective in the process of selection of a drive motor is to select the lightest motor that is compatible with the loading specifications. This objective has an important role in minimising motor weight. Moreover, it affects motor armature inertia, power dissipation and total power input to the motor. In this process, the allowable limiting factors are

- Maximum allowable energy dissipation in the armature over the load cycle,
- Maximum allowable output torque (at zero acceleration); generally limited by maximum allowable instantaneous torque of a motor, and
- Maximum allowable shaft speed.

Thus, torque, speed and temperature will be considered to be the basic limiting factors of an actuator motor. As is frequently the case in optimisation problems, all of these three factors enter the process in many situations. If the load motion characteristics are known, one can select the lightest possible motor with the desirable characteristics.

4.1.1 Manipulator motion

Broadly, the objective is to move the flexible manipulator from one position to another in the shortest possible time. In most material handling tasks, the velocity with which a robot end effector moves is constrained by the weight of the payload, weight of the manipulator

and the maximum amount of torque applicable to the hub of the manipulator. The choice of velocity profile will have an effect on motor weight. Other limiting factors affecting the design, typically, include

- Maximum acceleration for structural integrity of the manipulator and payload,
- Maximum velocity for safety.

Within these constraints, it is often desirable to minimise the total time of motion for a specific task. In the light of the discussion presented above, an approach to simplifying the problem is proposed here. The objective is an appreciation of what specification of motor is likely to be required for various classes of applications rather than a precise methodology for selection of a motor for a specific problem. To achieve this, the following assumptions are made:

- The single-link flexible manipulator under consideration is that shown in Figure 2,
- The torque supplied by the motor is τ_m and a known function of time. The maximum torque $\tau_{m\max}$ at the manipulator hub occurs during a period of maximum acceleration $\alpha_{m\max}$,
- Velocity profiles η_a are limited by the maximum acceleration of the manipulator $\alpha_{a\max}$ and maximum speed of the manipulator $\eta_{a\max}$, determined by external factors and the motor,
- The actuator motor operation is limited by a maximum instantaneous torque applied to the armature windings by the magnetic field and a maximum instantaneous shaft speed $\nu_{m\max}$.

However, in due consideration of heating and reliability, these limits should be set below the corresponding absolute maxima of the motor. The motor friction and winding losses are neglected so that the armature can be modelled as a pure inertia.

One of the results of the assumptions made above is the so called trapezoidal, or, in the case of short motions, triangular velocity profile as illustrated in Figure 3. As shown, velocity profile is divided into three parts: acceleration, run and deceleration. It may be apparent that the triangular profile is more efficient than the trapezoidal, as the run time in

the latter seems wasted. However, the energy dissipation in the motor armature for the trapezoidal one is 20.83% less than in the case of a triangular profile. Moreover, with the triangular velocity profile, the load is accelerated at a fixed rate and then decelerated at the same rate. This increases/decreases the velocity with time. As a velocity limit is associated with the system considered here, this method of excitation could not be used for larger angle movements.

4.1.2 Motor and gear ratio

An output torque from a gear box can be approximated as the torque applied to the armature by the magnetic field less the torque that is needed to overcome the inertia of the motor and the gear box. Assume that the inertia of the gear box can be neglected or reflected to the motor armature and/or reflected into the maximum armature torque $\tau_{a\max}$. Moreover, reflecting friction losses in the gear box and motor into $\tau_{a\max}$ yields

$$\tau_{a\max} = \tau_{m\max} N - J_m N^2 \alpha_{a\max} \tag{2}$$

where, N is the ratio of the motor speed to manipulator speed and J_m is the motor inertia. Temporarily assume that the objective is to pick N to minimise $\tau_{m\max}$ according to equation (2). Using a Lagrange multiplier λ, this is equivalent to minimising a performance index J_p.

$$J_p = \tau_{m\max} + \lambda\left(\alpha_{a\max} - \tau_{m\max} N + J_m N^2 \alpha_{a\max}\right)$$

This has a minimum at

$$\tau_{m\max} = 2 J_m N_2 \alpha_{a\max} \tag{3}$$

where, N_2 is the value of N that minimises $\tau_{m\max}$. Thus, equations (2) and (3) yield

$$\tau_{a\max} = J_m N_2^2 \alpha_{a\max} = 0.5 N_2 \tau_{m\max} \tag{4}$$

or,

$$N_2 = 2\left(\frac{\tau_{a\max}}{\tau_{m\max}}\right) \tag{5}$$

Substituting for N_2 from equation (5) into equation (4) yields

$$\tau_{a\max}\alpha_{a\max} = \frac{\tau^2_{m\max}}{4J_m} \tag{6}$$

In equation (6) the left-hand-side represents the performance characteristics of the manipulator whereas the right-hand-side represents the performance characteristics of the motor. This equation will be used later for sizing of the motor. When the gear ratio N_2 is used, the maximum motor velocity occurs at a time equal to $\nu_{a\max}/\alpha_{a\max}$ and the desired motor speed may exceed $\nu_{m\max}$. The gear ratio that minimises $\tau_{m\max}$ is N_1, where

$$N_1 = \frac{\nu_{m\max}}{\nu_{a\max}} \tag{7}$$

Replacing N in equation (2) by N_1 and substituting for N_1 from equation (7) yields

$$\tau_{a\max} = \tau_{m\max}\left(\frac{\nu_{m\max}}{\nu_{a\max}}\right) - J_m\left(\frac{\nu_{m\max}}{\nu_{a\max}}\right)^2\alpha_{a\max} \tag{8}$$

To obtain, the motor size, the terms representing the performance characteristics of the manipulator and of the motor should be separated. The maximum power that is required to be delivered by the motor is given by

$$P_{a\max} = \tau_{a\max}\nu_{a\max} \tag{9}$$

Substituting for $\tau_{a\max}$ from equation (8) into equation (9) yields

$$P_{a\max} = \left(\tau_{m\max}\nu_{m\max}\right) - J_m\nu^2_{m\max}\left(\frac{\alpha_{a\max}}{\nu_{a\max}}\right) \tag{10}$$

Equation (10) is the required relation giving the motor performance characteristics and the manipulator performance characteristics as separate terms. Let

$$\gamma_1 = \tau_{m\max}\nu_{m\max} \quad , \quad \gamma_2 = J_m\nu^2_{m\max} \tag{11}$$

Thus, using the above, equation (10) can be simplified as

$$P_{a\max} = \gamma_1 - \gamma_2\frac{\alpha_{a\max}}{\nu_{a\max}}$$

This gives the required maximum motor power with the gear ratio given by N_1. If the gear ratio is N_2 then the motor performance will be represented by

$$\gamma_3 = \frac{\tau_{m\max}^2}{4J_m} \tag{12}$$

This represents the maximum power rate of the motor. Thus, it follows from equation (6) that the motor power rate will be

$$RP_m \leq \gamma_3 \tag{13}$$

where, P_m is the required rate of power increase for the manipulator and is equal to $\tau_{a\max}\alpha_{a\max}$. The equality sign in equation (13) applies if the gear ratio is determined by the manipulator torque requirements $(N = N_2)$. If the gear ratio is determined by the manipulator speed requirements $(N = N_1)$ then as N_1 will be less than N_2, the motor power will be selected using equation (10).

In summary, if a flexible manipulator is required with an acceleration range of $\pm\alpha_{a\max}$ and speed range of $\nu_{a\max}$, then the gear ratio which yields the lightest motor is given by equations (5) and (7). When N_1 is the gear ratio, then the motor must meet the requirement

$$P_{m\max} \leq \left[\gamma_1 - \frac{\gamma_2}{T_a}\right] \tag{14}$$

where, $T_a = \nu_{a\max}/\alpha_{a\max}$. Similarly, when N_2 is the gear ratio, then the maximum manipulator power rate is given by

$$RP_{m\max} \leq \gamma_3 \tag{15}$$

It follows from equation (5) that the gear ratio (N_2) must be chosen so as to provide the required acceleration. However, this gear ratio may result in overspeed of the motor. If this happens, then equation (7) can be used to prevent the overspeed of the motor. Equations (6) and (7) are the necessary relations only for obtaining the gear ratio or coupling ratio.

Equation (14) gives the required motor power and equation (15) gives the required rate of motor power increase sufficient for the load requirements to be met. If N_1 is the gear ratio, the maximum power is achieved at full motor speed. If N_2 is the gear ratio then the motor never reaches full speed and the most demanding condition is associated with the ability of the motor to accelerate. Equations (14) and (15) thus provide the necessary and sufficient conditions for adequate motor capabilities for a specified manipulator design and performance.

The maximum manipulator power, $P_{a\max}$, and maximum manipulator power rate, $RP_{a\max}$, are functions of the manipulator characteristics and performance specifications. These are not related to the choice of the motor or gear ratio. These can be represented as

$$P_{a\max} = \tau_{a\max} \nu_{a\max}$$

and

$$RP_{a\max} = \tau_{a\max} \alpha_{a\max} \tag{16}$$

Equations (15) and (16) give the manipulator design and performance characteristics. Note that $\tau_{a\max}$ need not occur at $\nu_{a\max}$. However, it must occur during a period of $\alpha_{a\max}$. Equations (11) and (12) define the required motor characteristic parameters γ_1, γ_2 and γ_3. These are functions of the motor choice only and are not related in any way to the characteristics and performance specifications of the manipulator.

Frictional losses in the gear train and in the motor can be reflected back as part of the $\tau_{a\max}$. The parameters γ_1, γ_2 and γ_3 are in general monotonically increasing functions of weight for a given technology. Thus, to find the lightest motor among a set of motors, obtain γ_1, γ_2 and γ_3 for each and select the lightest which meets the inequality constraints of equations (14) and (15). Selection of $\nu_{a\max}$ and $\alpha_{a\max}$ has a strong influence on the motor size and motion times of the manipulator. The printed circuit armature type permanent magnet DC motor selected according to the design procedure above is a U9M4AT type (PMI Motion Technologies, 1988).

4.1.3 Advantages and disadvantages of gearing system

The main aim of introducing a gear system is to amplify the available torque from the actuator (here motor). Moreover, the use of such a system is motivated by other reasons as well. These are, to: (i) minimise power dissipation in the motor armature, (ii) minimise power input to the motor, (iii) maximise output torque to the load, (iv) match desired load speed to maximum motor speed. All of these four objectives are closely related to the objective of minimising the motor size for a given flexible manipulator load specification. Despite these advantages, gear systems have associated practical limitations. These are: (a) Addition of inertia at the hub. This inertia increases with gear ratio. (b) Addition of coulomb friction which, if too large, prevents or severely restricts back driving the actuator. Thus, the control of vibration of a flexible manipulator through the actuator, sometimes, becomes difficult. (c) Tendency to result in gross motions that are limited by the maximum speed of the actuator rather than the maximum torque. (d) Backlash. (e) Compliance.

Among the above, the effects (a) and (b) are especially severe for highly flexible manipulators, as these pose limitations on the controller to suppress higher frequency modes of vibration. Moreover, in non-direct drive robot manipulators, on average about 25% of the motor torque is spent in overcoming the joint friction (Craig, 1986). In multi-degree of freedom mechanical devices, coulomb friction causes additional non-linear coupling among the joints and is thus an additional contributor to the inaccuracies in the performance of a mechanical manipulator. Four causes of positioning errors, namely, gear transmission error, gear compliance, backlash and base motion have been identified (Whitney, et. al, 1986). It has been reported that actual trajectories of robot manipulators usually differ from the planned trajectories, particularly because of the effect of manipulator deflections and joint compliance (Tang and Wang, 1987). Effect (c) above will add at least one more parameter, determining the speed limitation and changing the nature of the gross motion time expectation to reflect a common speed over a large part of the gross motion cycle. Backlash, can result in undesirable instability in the response of the flexible manipulator or a limit cycle behaviour.

4.1.4 Hub friction

The characteristics of the frictional forces between two contacting surfaces often depend on several factors including the composition of the surfaces, the pressure between the two surfaces and their relative velocity. An exact mathematical description of the frictional forces is thus difficult to obtain. For practical purposes, however, frictional forces can be divided into three basic categories: viscous friction, static friction and coulomb friction (Kuo and Tal, 1978).

The static and coulomb friction depend upon the state of motion of the motor. Static friction Fs appears when the motor is not in motion but is tending to move . As the motor begins to rotate, the friction drops to coulomb friction Fc. The static and coulomb friction are each sometimes called constant friction. In the flexible manipulator system considered here the frictional losses are only contributed by the motor. The amount of friction associated with the motor is determined experimentally, so that the extent of the problem involved can be visualised. The experimental set-up for the motor friction measurement is shown in Figure 4. Figure 5 shows the, experimentally determined, torque as a function of shaft velocity. The values of Fs, Fc and the viscous coefficient B thus obtained are $0.011Nm$, $0.01Nm$ and $0.029mNm/rad/\sec$ respectively.

4.2 Drive amplifier

Amplifiers used to drive DC motors for motion control systems can broadly be classified as linear and switching amplifiers. From a control viewpoint, a linear amplifier is desirable, since it has linear characteristics with no significant control lag within the operating bandwidth. However, a significant amount of power is dissipated in the output transistor of such an amplifier, especially with the motor under low-speed, high-torque conditions where the motor back emf is low and the current is high. This is a marked contrast to switching amplifiers. Switching amplifiers control the motor voltage by varying the duty cycle of the voltage applied to the motor and operate in either a saturated or off mode and dissipate little power in either state, giving rise to efficient operation. However, electromagnetic interference (EMI) problems are often severe with these motors, and the

system tends to be more complex and failure prone. Thus, there is no clear cut superiority of one type of amplifier over the other.

In general, linear amplifiers are preferred in wide-bandwidth, low-power systems. They are ideal in driving low inertia motors, where high acceleration currents are required for short time intervals. Conversely, switching amplifiers are usually used in larger systems, especially those which require extended operation at low speed and high torque, where the power dissipation of a linear amplifier would be high. In the flexible manipulator system considered here, a switching mode amplifier is selected for power input considerations. The associated EMI, as discussed later, introduces noise in the sensitive transducer circuitry. With due consideration of these circumstances, a linear drive amplifier was selected which can also be used as a servomotor in velocity position or torque control mode. This is an LA5600 type amplifier (Electrocraft Corporation, 1985). A Connection diagram of the amplifier with the flexible manipulator system and clamping system is shown in Figure 6.

The main objective here is to use the drive amplifier as a current amplifier to drive the motor. The input voltage and produced torque relationship of the amplifier for input scaling resistors of 4 kΩ and 7.4 kΩ as obtained experimentally are shown in Figure 7. It is noted that the relationship is linear through the operating range of interest.

It is important, for monitoring and control purposes, to measure the applied torque at the hub of the manipulator. There are various types of torque transducers that are commonly used for such purposes. These mostly utilise strain gauges as active elements. Optical methods, where a light beam is modulated by the applied torque and the electrical output from the photovoltaic detector provides torque information through the shaft, have also been used recently to measure the torque.

The motor drive amplifier has a voltage output proportional to its current output. This, for known voltages, will allow the calculation of the amount of current output to the motor and hence the torque applied to the hub of the manipulator. To avoid further inertia at the hub and additional amplifier, this MCO output is used as an indication of the applied torque at the hub. Experiments were carried out to compare the experimentally measured

and calculated output currents using the MCO voltage. The amount of developed torque was also measured using a spring balance. These are shown in Figure 7. It follows from this result that

- The MCO voltage represents the actual current output of the amplifier.
- The amplifier input voltage and the torque produced by the motor are linearly related.
- The motor torque constant specified by the manufacturer is reliable. The difference between the measured and calculated torque is noticeable outside the range $(-0.3,+0.3)Nm$. However, the torque requirement in the case of the flexible manipulator system under consideration is well within this range.

4.3 Hub angle sensor and processing circuit

To control the rigid body motion of the flexible manipulator, the angular position is required to be measured at the hub. There are two methods commonly used for measurement of angular position of a shaft: (a) employing a rotational potentiometer on the shaft of the motor, (b) using an optical shaft encoder. Method (b) gives a direct digital output. However, it requires further processing circuitry for direct interfacing with the computer bus. The potentiometer method of measuring angular rotation is a troublesome one, due to the inherent noise associated with the potentiometer. Thus, following a process of studying various available shaft encoders, a suitable one with a resolution of 2048 pulses/revolution was selected. The selection process has been mainly concerned with the size and pulses/revolution of the shaft encoder. The pulse/revolution can be increased by four times if the incremental encoder interface (IEI) chip operates in a quadruple mode, in which case the end-point positioning accuracy increases to 0.736 mm. To allow gather angular position information in analogue form, a precision interface circuit was thus developed to convert the shaft encoder output to an analogue signal. The circuit mainly consists of a TCHT2000 IEI chip (Texas Instuments, 1990) and an MP7636A double buffered 16-bit multiplexing D/A converter (Micro Power Systems, 1990). A block diagram of the system is shown in Figure 8. The TCHT2000 can determine the direction

and displacement based on two input signals (Ua1 and Ua2) from the shaft encoder. The MP7636A incorporates a unique bit decoding technique yielding lower glitch, higher speed and excellent accuracy over temperature and time. It provides 16-bit data loading through eight input data lines for direct interface to 8-bit data buses. The output of the D/A converter is amplified through a scaling amplifier, with $\pm 90^0$ rotation scaled to ± 8.15 volts DC output.

4.4 Hub velocity sensor and amplifier

Three methods of angular velocity measurement are in common use. These are (a) tachogenerator method, (b) electromagnetic pulse method, and (c) opto-electronic method. Among these, due to cost effectiveness and from an application viewpoint, the iron core or moving coil type tachogenerators are more popular for measurement of the angular velocity (Hastings, 1986; Kotnik, et. al, 1988). Velocity measurement can be obtained by differentiating the output signal from the angular displacement transducer. This process of differentiation, however, will amplify any noise in the measurement signal and thus is not reliable.

A conventional type tachometer which is mounted on the shaft of the driving motor was found to produce a considerable amount of ripple due to its commutation effect. To overcome this problem, a velocity transducer was purpose designed for this application using the existing tachometer principle. The flexible manipulator under consideration can rotate up to 180^0. A circular shape permanent magnet with an active range of about 240^0 and a moving coil around it was then specified for the velocity transducer. A moving coil permanent magnet ammeter provides the basis for this. The inertia of the moving coil is negligible in comparison to the motor inertia. The meter was mounted on a circular ring and then attached to the motor body so that the motor shaft was in line with the centre of the moving coil. Finally the motor shaft was attached to the moving coil in a novel manner, enabling the moving coil to rotate with the motor shaft around the permanent magnet. The moving coil can, thus, produce a voltage which is proportional to the velocity of the shaft

and is free from any ripple. The output of this coil is amplified using a differential amplifier and a scaling amplifier. The gain of the scaling amplifier is made variable for adjustment purposes. To check the uniformity of the output voltage developed throughout the range of angular movement, the system was excited using sinusoidal input from a signal generator, with the hub placed at various angle positions. The developed output from the velocity measurement system was also recorded for various positions. A comparison of these outputs for various hub positions showed a very small difference (about 0.1%) leading to the conclusion that the voltage developed by the velocity sensing system is uniform throughout the range of angular movement. Calibration of the developed velocity measurement system is not straightforward. This is due to its restricted angle of movement. To overcome this, an optical velocity measurement system was used with the existing tachometer for the calibration procedure.

4.5 Strain gauge and amplifier

To obtain direct modal information, the bending strain on the manipulator during its motion needs to be measured. Although, there are excellent non-electrical devices of measuring this vibration, a wide range of electrical strain gauges are still commonly used due to their practical advantages (Haslam, et. al, 1981). The advantages of electrical resistance strain gauges are: high accuracy, fast speed of response, good linearity and stability, smallest possible size, cost effectiveness and extended range of operation. The nature of the experiments involved, requiring precise and fast measurement of strain, makes these devices suitable candidates. When the manipulator flexes the strains on opposite sides of the manipulator are of equal magnitude and opposite signs and the resistance of one strain gauge increases while that of the other falls. Over a wide range, the change in resistance is linearly proportional to strain and hence the difference in the two resistances gives a direct measure of the strain in the manipulator.

A foil type strain gauge CEA-13-250UW-350 was selected in this design (Micro Measurements, 1982, 1983a). Making accurate and reliable strain gauge measurements

does not depend on the quality of the strain gauge alone. The gauge can perform to its fullest potential only if the installation is of comparable quality (Micro Measurements, 1983b). Measurement of strain will be performed at four locations (1, 2, 3 and 4) along the manipulator; location-1 being closest to the hub and location-4 to the end-point. The specific implementation of strain gauges for the experiment carried out here consists of two active gauges in each location connected in half bridge configuration, as commonly used for measuring planar bending of a beam. This configuration is much less sensitive to stresses due to torsion, extension and transverse bending and provides higher signal levels with bending than an individual gauge.

To amplify the strain gauge output, a strain gauge amplifier chip was selected. This is a purpose designed, hybrid, low noise, low drift, linear DC amplifier. A block diagram of the strain gauge amplifier set-up is shown in Figure 9. The performance of the measurement system is examined by locking the joint and deflecting the end-point in fixed increments. These are shown in Figure 10 for location 1 and 4 along the manipulator. These results are compared against linear elastic theory, allowing for calibration of the bridge and amplifier in one step.

4.6 Measurement of hub inertia

Hub inertia is an important component, influencing the required torque for a specified movement as well as the frequency of vibration of the manipulator. Due to the irregular shape of the hub, it is difficult to calculate its inertia theoretically with reasonable accuracy. Thus, an experimental method is used to obtain the hub inertia. This is based on applying a current to the motor comprising a DC bias and a sinusoidal component (Kuo and Tal, 1978). The resulting motor velocity and motor current are then measured. The values of peak current i_p and peak velocity v_p are obtained. As the value of the torque constant K_t and frequency of applied signal f are known, the total inertia of the hub and the motor armature can be calculated using $J = \frac{K_t i_p}{2\pi f v_p}$. The DC component of the current

is adjusted so that the motor runs in the same direction, although its velocity is modulated sinusoidally.

To avoid the static and dynamic friction, a DC component was added to keep the motor running in the same direction. The effects of viscous damping were minimised by keeping the amplitude of the velocity change at the lowest level. For increased accuracy, several measurements were taken at different frequencies.

4.7 Accelerometer and amplifier

To monitor the end-point vibration of the flexible manipulator, an accelerometer is used. As the manipulator is light in weight, the accelerometer to be used should be as light and small as possible to reduce its effect on the manipulator vibration characteristics (Mace, 1991). Various types of accelerometer are in common use. A miniature integrated circuit piezoelectric (ICP) accelerometer was selected here. The characteristics of this accelerometer cover the dynamic range of interest of the manipulator system. Moreover, it has a built-in FET source follower which lowers the output impedance level. The low impedance output allows the use of long cables without an appreciable signal loss or distortion and further avoids the use of low noise cables.

The features of the main amplifier unit used include the powering of transducer electronics, debiasing the output signal from the transducer, amplification of the signal and indication of normal and faulty system operation. The accelerometer was mounted at the end-point using epoxy adhesive. Special care was taken in fixing the accelerometer, as thickness of the wax, any external particle or improper surface preparation will affect the frequency response characteristics of the system.

5 Practical constraints

There are three major areas where problems were incurred: (a) noise/interference, (b) gearbox and (c) torque measurement system. To minimise the interference level in transducer and instrumentation systems, fundamental precautions in the system design

were taken. These included optimum wiring technique, shielding and impedance matching. Despite all these precautions, there was a considerable amount of noise at the output of the transducer amplifiers due to their required high gain configuration. Following a close investigation, two sources of noise were identified: (1) the AC mains power to the amplifier via ground and electromagnetic means, (2) the pulse width modulated amplifier used for driving the motor. This type of amplifier produces an intense electromagnetic field due to its inherent high frequency oscillation.

To solve the first problem the amplifier circuit was double shielded and the AC power source was replaced with a battery to power the amplifier circuit. The interference from the switching amplifier was of such magnitude that, even after double shielding the switching amplifier and transducer amplifiers, a considerable amount of noise appeared at the amplifier output. Thus, the switching mode amplifier was replaced with a linear amplifier. This eliminated the noise problem.

After assembling the structure according to the initial design (see Figure 11) it appeared that the gearbox was introducing considerable amount of backlash and, thus, producing additional vibration in the flexible manipulator. This induced vibration had a component within the range of vibration frequency of the flexible manipulator. Thus, modelling and control of the system with this gearbox would require consideration of this additional vibration, increasing the complexity of the controller. Moreover, the gearbox had a considerable amount of inertia relative to the flexible manipulator hub. This would increase the response time of the system considerably. To overcome these problems, the mechanical structure was redesigned without the gearbox. However, it is worth noting that there exists a gearbox, the so called Cyclo gearbox which has low inertia, high efficiency and low or zero backlash that could be a suitable candidate for this application.

Measurement of the applied torque to the hub is important for successful vibration control. There are different types of commercial torque transducers available. However, the measurement range of these transducers are relatively high and, thus, cannot be used for torque measurement with reasonable accuracy. Therefore, a special torque measurement system was initially designed (see Figure 11) in which the motor tachometer

and gearbox shaft were placed on a frictionless bush and the movement of the motor gearbox assembly with respect to the mounting structure was measured to obtain the applied torque to the hub. A steel ring was clamped around the gearbox and a spring steel bar was used to clamp the steel ring to the mounting structure. A pair of strain gauges was placed on the spring steel bar to measure the strain. The measured strain was then calibrated for torque measurement.

The strain/torque relationship was found to be linear within the range of interest. However, there was a considerable amount of friction between the bush and the mounting structure which introduced a backlash in the measurement system. Therefore, the torque was instead measured from the motor drive amplifier output current, as stated earlier.

6 Computer, interfacing and software

The computer used for this experimental set-up is an 80286 based microcomputer, with 2 Mbytes of RAM and 64 Mbytes of Hard disk. Data acquisition and control is accomplished through the utilisation of an RTI-815 I/O board. This board can provide a direct interface between the microcomputer and the actuator and transducers for a variety of data acquisition, analogue output, digital I/O and time-related digital I/O applications (through AM9513A counter/timer chip). The system was later upgraded to a Viglen PC compatible with the IBM PC(AT). This employs a 32-bit 80486 processor, 40487 co-processor and 4 Mbytes of RAM with 50 MHz clock speed.

The RTI-815 board contains a single 12-bit A/D converter with a conversion speed of 25 μsec. Various configurations of its CMOS multiplexer enables it to receive different numbers of input channels with different voltage levels. A/D conversion can be initiated by one of three possible sources: using a software convert command, applying an external TTL logic level signal or by programming the AM9513A counter/timer chip. The RTI-815 is able to generate an interrupt when one of three independent conditions has occurred: when an A/D conversion is completed, when an overrun condition has occurred or when a given number of counts has finished.

The board contains two independent voltage output channels, each with its own 12-bit D/A converter, that can produce an output of 0 to +10V or ±10V. Output settling time is 20 μsec for full scale step changes. The board also provides an 8-bit (eight channel) non-latching parallel digital input port and an 8-bit latching parallel digital output port.

For time related digital I/O applications, the AM9513A counter/timer chip provides the RTI-815 with three independent 16-bit channels that can be used for such counter/timer functions as event counting, frequency measurement, single pulse output and time proportional output.

The board is mapped into the I/O channel structure of the microcomputer as a block of 16 consecutive bytes. A combination of PASCAL and assembly language is used for data acquisition using DMA.

7 Conclusion

The design and development of a flexible manipulator system has been presented. This has been divided into three stages: (a) design and construction of the mechanical structure, (b) choice of suitable transducers, (c) development of the required amplifier and processing circuits and their calibration.

Details of the selection of a suitable flexible manipulator for a given specification have been given. In the design of the drive actuator, several options have been considered. This has lead to the selection of a printed circuit armature type motor due to its low inertia, low inductance and physical structure. The selection criteria for a suitable gear box ratio has been developed. Although, due to the problem of backlash and inertia, a gearbox has not been used, the developed relations could easily be used, e.g. with a Cyclo type gearbox.

The amplifier/controller for driving the motor has been selected with due consideration of its several features such as motor clamping, directional clamping and provision of output current monitoring. For measurement of angular movement, the developed processing circuit is able to produce both digital and analogue outputs at the same time. This enables the use of analogue output from 16-bit D/A as a feedback signal

to the amplifier/controller and digital output to the computer. A new type of velocity measurement transducer has been used instead of the conventional tachometer. A special feature of this transducer is that the output is free from any noise induced from commutator friction. Moreover, the inertia of this system is very small. In the design related to the choice of accelerometer and strain gauge the size, weight and frequency range constraints have been considered strictly. The accelerometer selected incorporates a built-in FET source follower which allows for a lower output impedance level.

Due to the irregular shape of the hub, the hub inertia has been measured experimentally. Motor friction has also been measured experimentally to verify the supplier data-sheet. Various problems incurred during the construction and testing of the experimental system. These included noise/interference due to the AC mains supply, backlash and inertia due to the gearbox and stiction due to the initially designed torque measurement system. The problems, thus, identified have been dealt with accordingly and their effects eliminated.

8 Acknowledgement

The authors would like to thank Mr G G Nicklin for his assistance and support in the construction of the system.

9 References

BOOK, W. J. (1974). *Modelling, design and control of flexible manipulator arms*, PhD thesis, Department of Mechanical Engineering, MIT, USA.

CHANG, L. W. and CANNON, K. P. (1990). A dynamic model on a single link flexible manipulator, *Transaction of the ASME Journal of Vibration and Acoustics*, **112**, (1), pp. 138-143.

CRAIG, J. J. (1986). *Introduction to robotics: Mechanics and control*, Addition-Wesley, Reading, USA.

CRITCHLOW, A. J. (1985). *Introduction to Robotics*, Macmillan, New York.

ELECTROCRAFT CORPORATION (1985). *DC motors speed controls servo systems*, Fifth edition, Electrocraft Corporation/Robbins & Mayers.

FURUYA, Y. and SHIMADA, H. (1991). Shape memory actuators for robotic applications, *Materials and Design*, **12**, (1), pp. 21-28.

FURUYA, Y., SHIMADA, H., GOTO, T. and HONADA, R. (1987). An extreme operation robot designed to develop the deep submarine managanese nodules resources, *Proceedings of Symposium International Co-Operation on Industrial Robots, SICIR-87, Tokyo*, p. 261.

HASLAM, J., SUMMERS, G. R. and WILLIAMS, D. (1981). *Engineering instrumentation and control*, Edward Arnold Publishers Ltd.

HASTINGS, G. G. (1986). *Controlling flexible manipulators: An experimental investigation*, PhD thesis, Georgia Institute of Technology, USA.

HASTINGS, G. G. and RAVISHANKAR, B. N. (1988). An experimental system for investigation of flexible links experiencing general motions, *Proceedings of Conference on Decision and Control*, pp. 1003-1008.

HIROSE, S., IKUTA, K. and UMETANI, Y. (1986). Development of shape memory alloy actuator (Performance evaluation and new configuration method), *Journal of Robotic Society, Japan*, **4**, (2), p. 15.

HIROSE, S., OITA, K. and TSUKAMOTO, M. (1984). Three dimensional active endoscope actuated by shape memory effect, *2nd Japan Robot Symposium*, p. 123.

INLAND MOTORS (1985). *Direct drive DC motors*, Inland Motors, USA.

KHOSLA, P. K. and KANADE, T. (1988). Experimental evaluation of nonlinear feedback and feedforward control schemes for manipulators, *International Journal of Robotics Research*, **7**, (1), PP. 790-798.

KLAFTER, R. D., CHMIELEWSKI, T. A. and NEGIN, M. (1989). *Robotic engineering: An integrated approach*, Perntice-Hall, Englewood Cliffs.

KOTNIK, P. T., YURKOVICH, S. and ÖZGUNER, Ü. (1988). Acceleration feedback for control of a flexible manipulator arm, *Journal of Robotics Systems*, **5**, (3), pp. 181-196.

KUO, B. C. and TAL, K. (editors) (1978). *DC motors and control systems*, SRL Publishing Company, Illinois.

MACE, B. R. (1991). The effects of transducer inertia on beam vibration measurements, *Journal of Sound and Vibration*,**145**, (3), pp. 365-379.

MICRO MEASUREMENTS (1982). *Technical note TN-508: Fatigue characteristics of strain gauges*, Welwyn Strain Measurements, UK.

MICRO MEASUREMENTS (1983a). *Technical note TN-505: Strain gauge selection criteria*, Welwyn Strain Measurements, UK.

MICRO MEASUREMENTS (1983b). *Catalogue A-110-4: M-line strain gauge accessories*, Welwyn Strain Measurements, UK.

MICRO POWER SYSTEMS (1990). *Data sheet for MP7636A, CMOS double buffered 16-bit multiplexing D/A converter*, Micro Power Systems, California.

PMI MOTION TECHNOLOGIES (1988). *General application of printed motors*, PMI Motion Technologies, New York.

TANG, S. C. and WANG, C. C. (1987). Computation of the effects of link deflections and joint compliance on robot positioning, *Proceedings of the IEEE Conference on Robotics and Automation*, pp. 910-915.

TEXAS INSTRUMENTS (1990). *Data sheet for THCT-2000, incremental encoder interface*, Texas Instruments, USA.

WHITNEY, D., LOZINSKI, C. and ROURKE, J. (1986). Industrial robot forward calibration method and results, *Transactions of ASME - Journal of Dynamics Systems, Measurement and Control*, **108**, (1), pp. 1-8.

YEAGER, Y. (1984). A practical shape memory electromechanical structure, *Mechanical Engineering*, **106**, pp. 52-55.

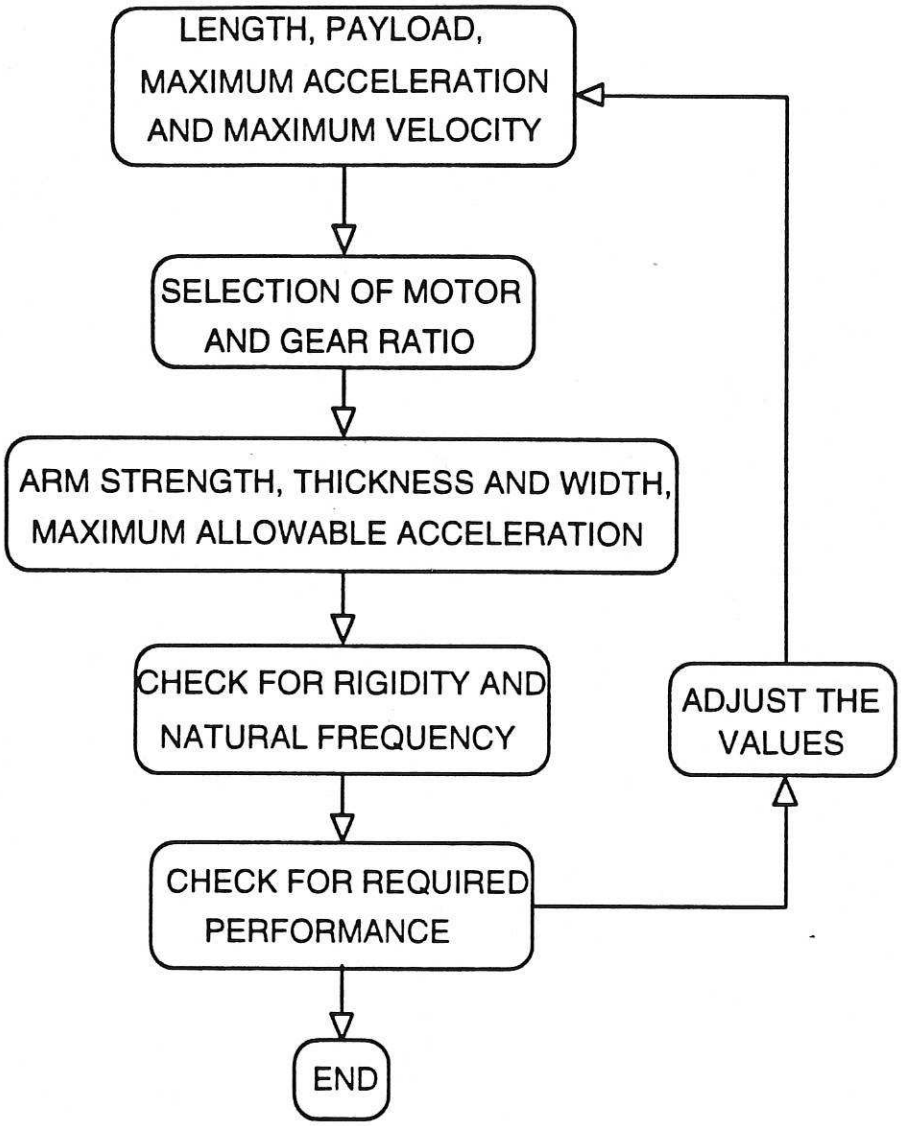

Figure 1: Flexible manipulator design steps.

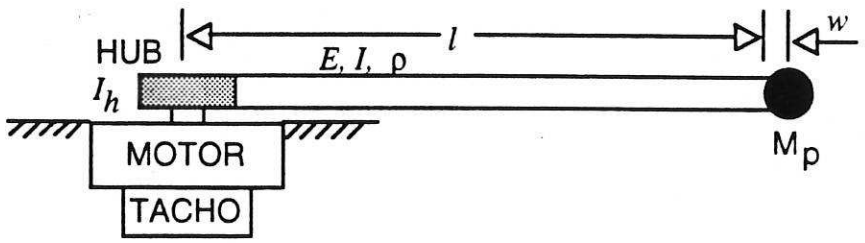

Figure 2: Outline of the flexible manipulator system.

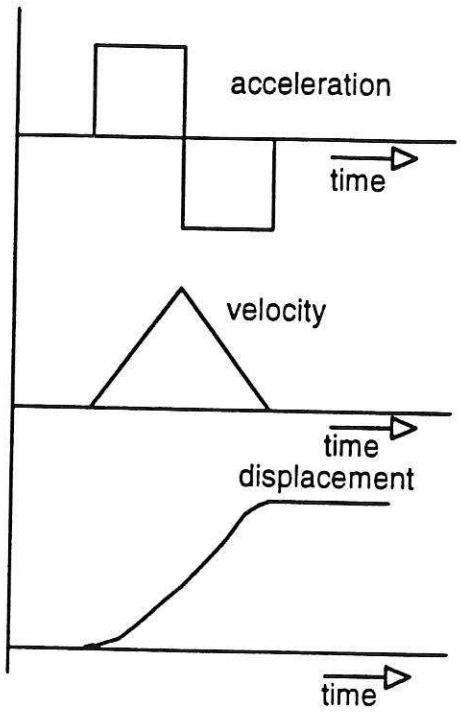

(a)

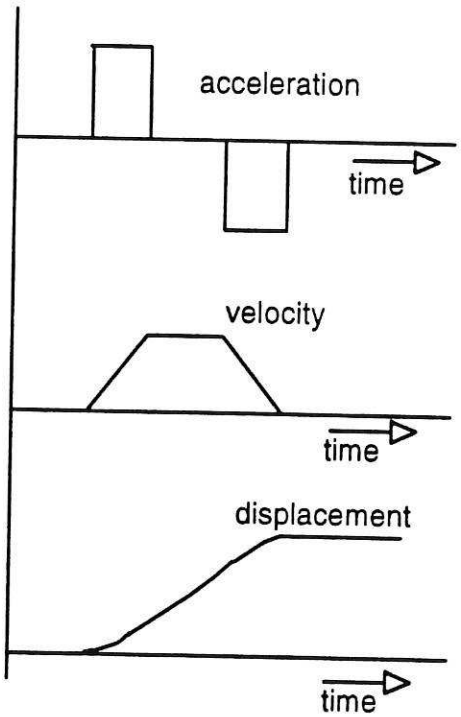

(b)

Figure 3: Different velocity profiles for flexible manipulator movement;
(a) Triangular profile.
(b) Trapezoidal profile.

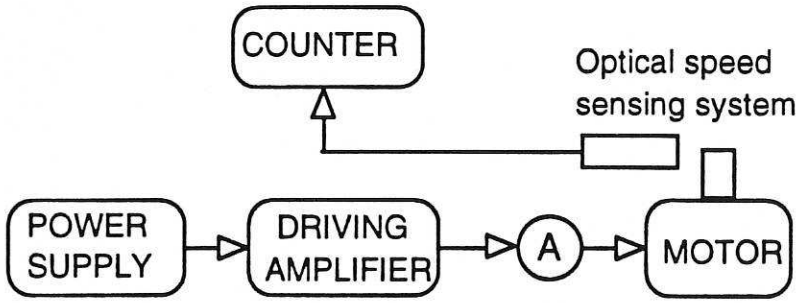

Figure 4: Connection diagram for motor friction measurement.

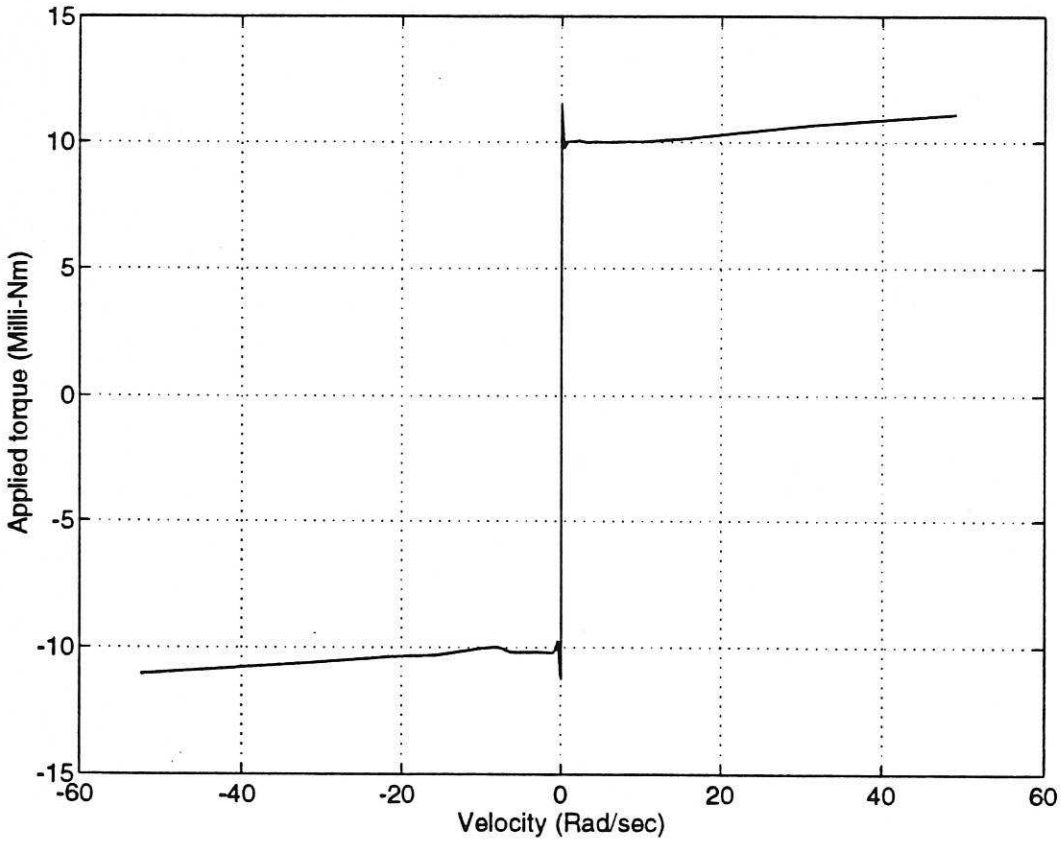

Figure 5: Experimentally measured static and dynamic friction characteristics of the U9M4AT motor.

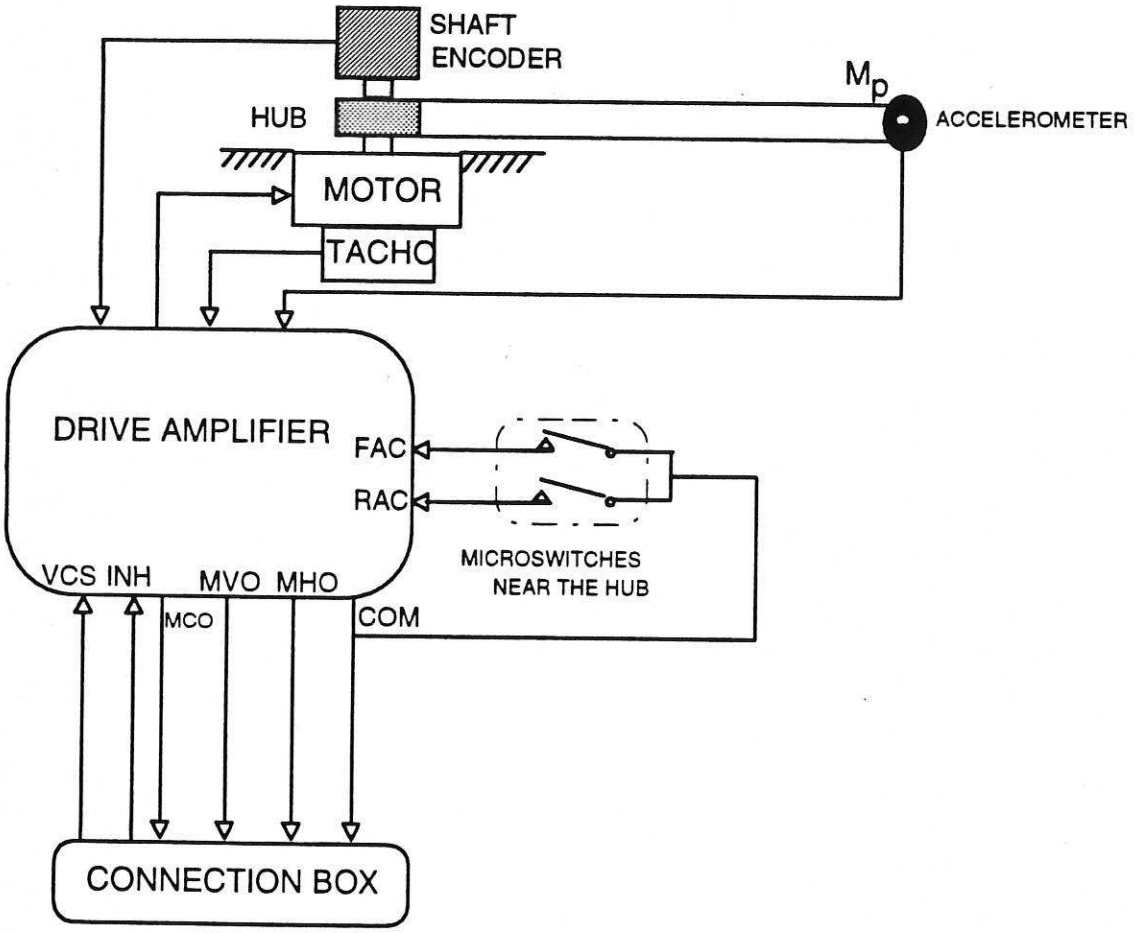

Figure 6: Connection diagram of the motor amplifier with the flexible manipulator system.

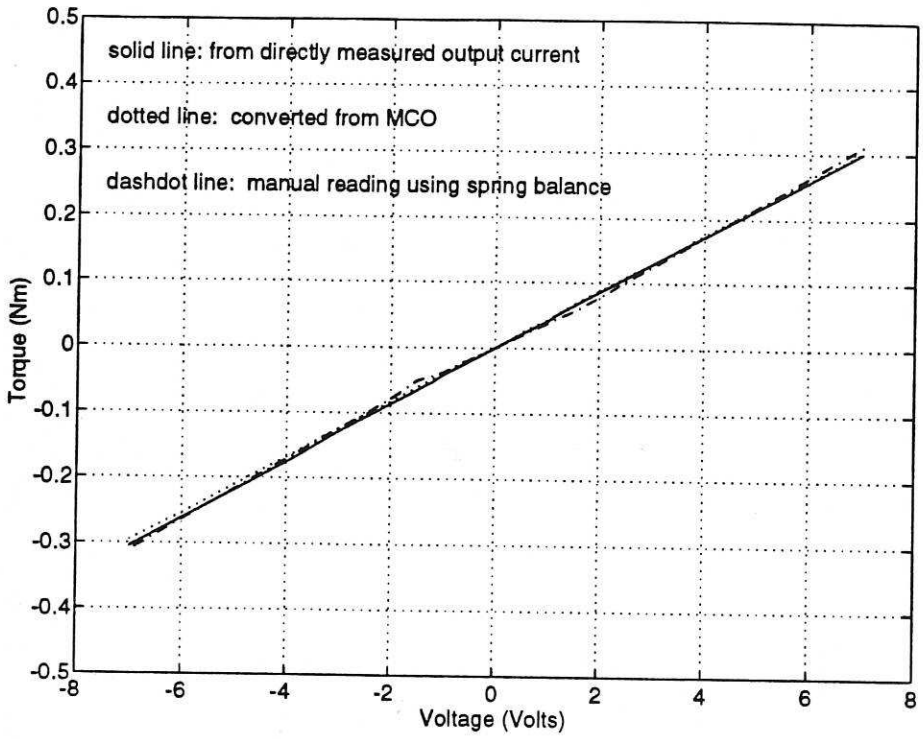

(a)

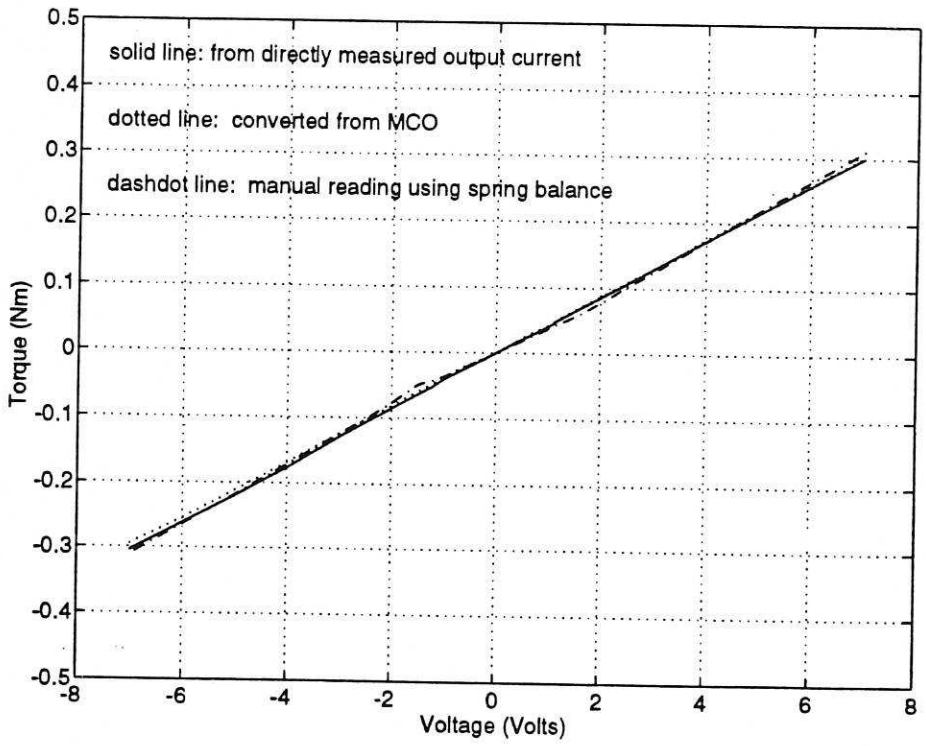

(b)

Figure 7: Produced torque as a function of amplifier input voltage;
(a) Input scaling resistor at 4 kΩ.
(b) Input scaling resistor at 7.4 kΩ.

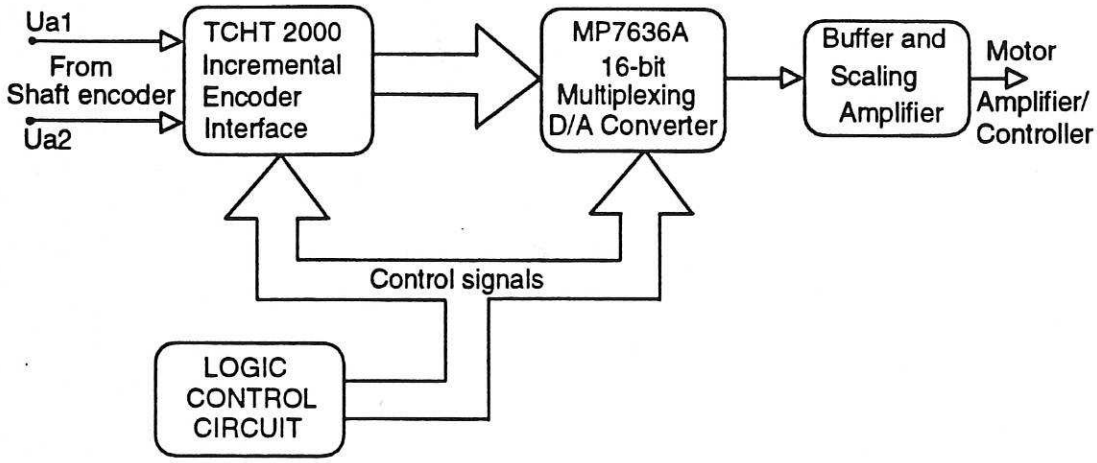

Figure 8: Block diagram of the conversion of shaft encoder output to analogue form.

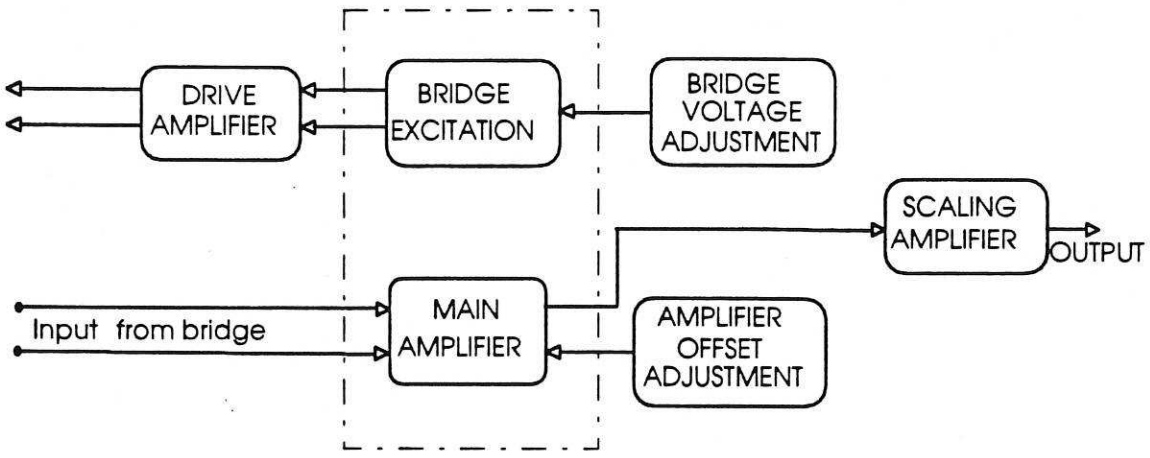

Figure 9: Block diagram of the strain gauge amplifier system.

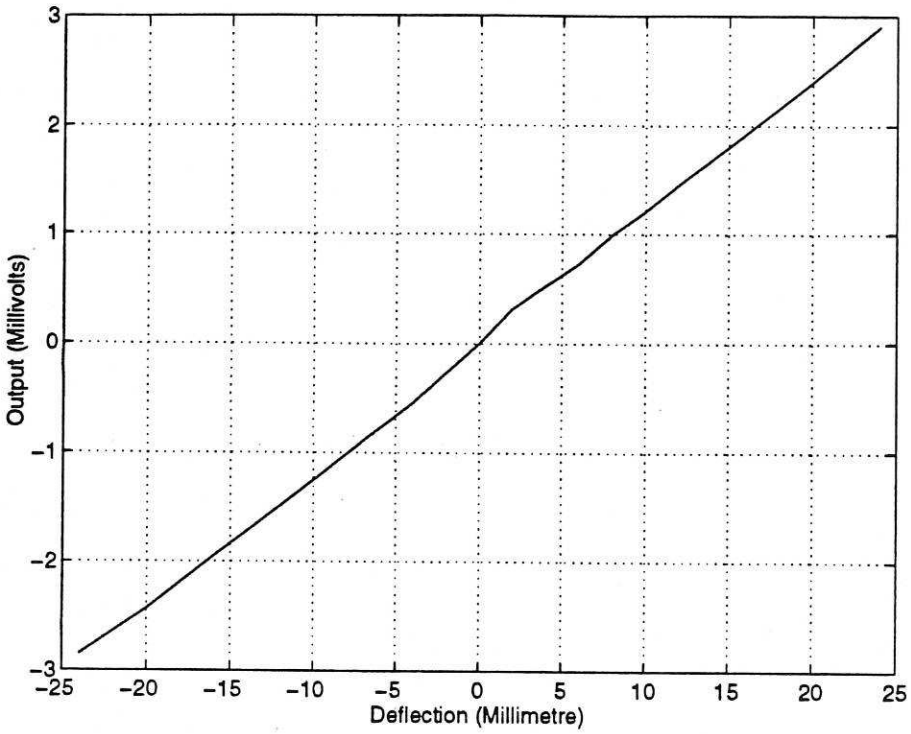

(a)

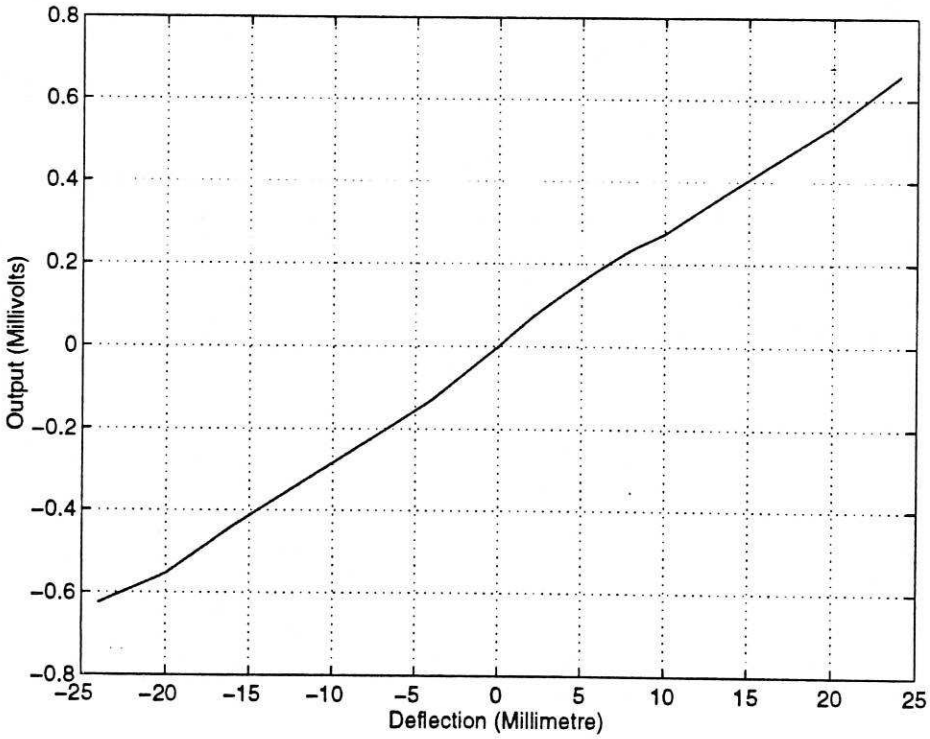

(b)

Figure 10: Strain gauge amplifier output as a function of deflection;
(a) Location-1.
(b) Location-4.

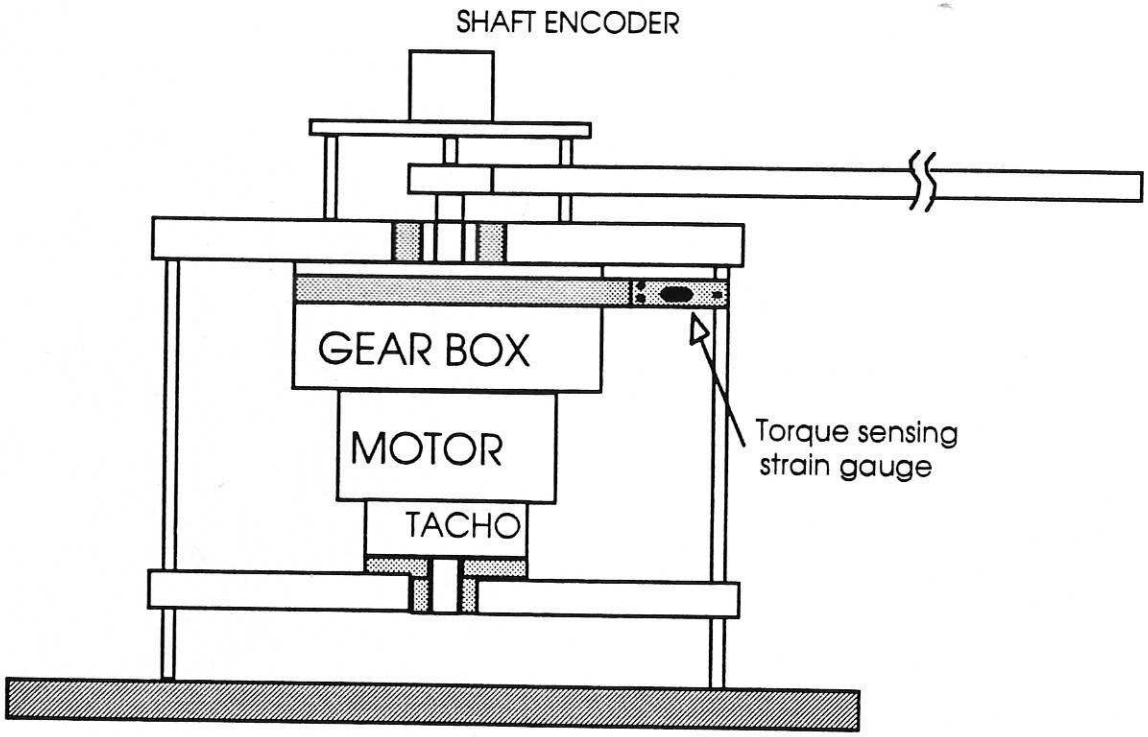

Figure 11: Outline of the initial structural design of the flexible manipulator system.